Journal of Medicinal Chemistry

Article

pubs.acs.org/jmc

Tetrahydropyrroloquinolinone Type Dual Inhibitors of Aromatase/Aldosterone Synthase as a Novel Strategy for Breast Cancer Patients with Elevated Cardiovascular Risks

Lina Yin,[†,‡] Qingzhong Hu,[†] and Rolf W. Hartmann*[,†]

[†]Pharmaceutical and Medicinal Chemistry, Saarland University & Helmholtz Institute for Pharmaceutical Research Saarland (HIPS), Campus C2-3, D-66123 Saarbrücken, Germany

[‡]ElexoPharm GmbH, Campus A1, D-66123 Saarbrücken, Germany

Supporting Information

ABSTRACT: The application of aromatase inhibitors to postmenopausal breast cancer patients increases the risk of cardiovascular diseases (CVD), which is believed to be caused by the abnormally high concentrations of aldosterone as a consequence of the estrogen deficiency. Dual inhibitors of aromatase (CYP19) and aldosterone synthase (CYP11B2) are therefore proposed as a novel strategy for the adjuvant therapy to reduce the CVD risk for these patients. By combining decisive structural features of CYP11B2 and CYP19 inhibitors into a common template, a series of pyridinylmethyl substituted 1,2,5,6-tetrahydro-pyrrolo[3,2,1-*ij*]quinolin-4-ones were designed and synthesized. Interestingly, the substituents on the methylene bridge showed strong influences on the inhibitory activities leading to opposite effects, that is, a given substituent showed an increase in inhibition of one enzyme, while it led to a decrease for the other enzyme. The compromise of this conflict led to compounds **3j**, **3k**, **3n**, and **3p** as potent and selective dual inhibitors of CYP19 and CYP11B2, especially compound **3p**, which exhibited IC_{50} values of 32 and 41 nM for CYP19 and CYP11B2, respectively, and a high selectivity toward CYP17 and CYP11B1. This compound is considered as a candidate for further evaluation in vivo.

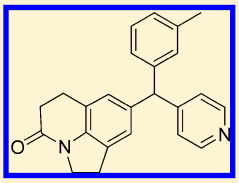

INTRODUCTION

Estrogens not only act physiologically as important sexual hormones to promote the development of female secondary sexual characteristics and to maintain the functions of the reproductive system but also exhibit dichotomous impacts on human health under some pathological circumstances. On the one hand, estrogens stimulate the proliferation of breast cancer (BC) cells that are estrogen receptor (ER) or progesterone receptor (PgR) positive.[1] Estrogen deprivation is therefore a rational treatment for BC. Two approaches have been implemented in clinic: selective estrogen receptor modulators[2] and aromatase (CYP19) inhibitors, such as letrozole and vorozole (Chart 1). Since CYP19 inhibitors show fewer side effects especially in long-term application, they are first choice nowadays as adjuvant therapeutics for postmenopausal breast cancer patients. On the other hand, estrogen deficiency is correlated with cardiovascular disease (CVD), which has been demonstrated by the fact that the incidence of CVD in postmenopausal women is triple that of premenopausal women at the same age.[3] Estrogens have been proven to exhibit protective effects on heart[4] and kidney.[5] The administration of estrogen prevents heart failure after myocardial infarction[6] and attenuates ventricular hypertrophy and remodeling.[7] As for BC patients, menopause and the application of CYP19 inhibitors decrease plasma estrogen concentrations to undetectable levels,[8] which leads to an even higher risk of CVD.

It is believed that the high CVD risk resulting from estrogen depletion is caused to a great extent by an increase of the aldosterone levels. The estrogen deficiency not only directly promotes aldosterone secretion but also upregulates other components of the renin−angiotensin−aldosterone system (RAAS) such as renin, angiotensin II, angiotensin converting enzyme, and angiotensin type 1 receptor, which further elevate the aldosterone biosynthesis.[9] The abnormally high concentrations of aldosterone cause retention of sodium and water, leading to an increase of blood volume and the subsequent elevation of blood pressure.[10] It also promotes the influx of calcium into vascular smooth muscle cells[11] and the expression of adrenomedullin and regulator of G protein signaling-2,[12] leading to vasoconstriction, which together with the increase of blood volume results in chronic hypertension. Moreover, excessive aldosterone acts as a pro-inflammation factor[13] and induces the production of reactive oxygen species (ROS).[14] Inflammation and ROS formation lead to cardiac myocyte necrosis, collagen synthesis, and fibroblast proliferation, thus resulting in cardiac and vascular fibrosis and an increase in myocardial stiffness.[15] Subsequently, cardiac hypertrophy and ventricular remodelling occur as further structural deterioration with functional degradation proceeds.[16] The ventricular remodeling causes diastolic dysfunction, diminishes contractile capability, reduces the stroke volume, and ultimately results in heart failure, often leading to sudden death.

Aldosterone synthase (CYP11B2) is the crucial enzyme catalyzing the conversion of 11-deoxycorticosterone to aldosterone. Its inhibition, leading to a reduction of aldosterone levels, would be beneficial for postmenopausal BC patients under CYP19 inhibitor treatment. Instead of a combination therapy with inhibitors of

Received: September 27, 2012
Published: January 3, 2013

Chart 1. Design Concept of Dual CYP19/CYP11B2 Inhibitors

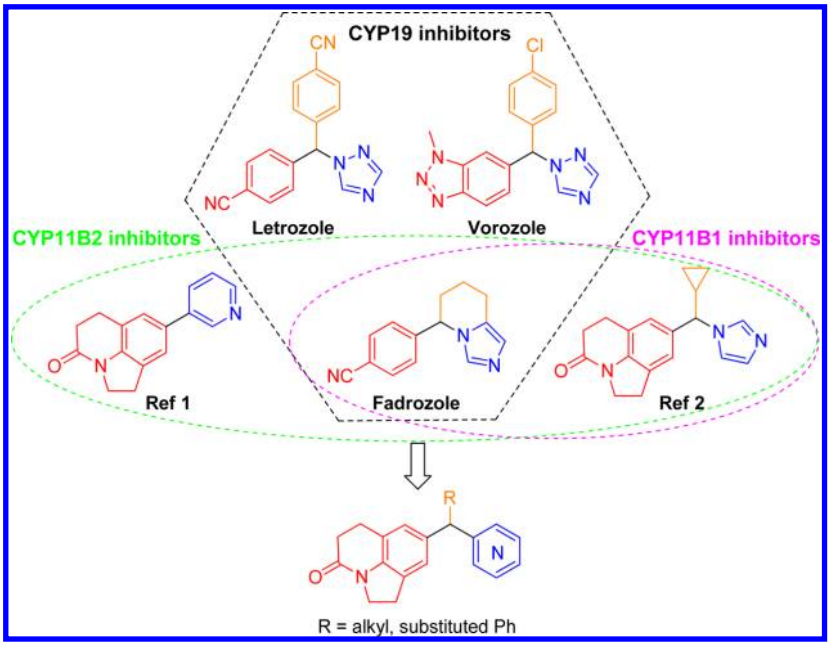

CYP11B2 and CYP19, dual inhibitors of both enzymes would be advantageous for a better compliance and for decreasing side effects. Besides, application of this kind of dual-target-directed agent[17] could also avoid drug−drug interactions often observed after the administration of two drugs in combination. Accordingly, we would like to develop dual inhibitors of both enzymes as an innovative approach for the treatment of BC. Important structural features of known CYP11B2 and CYP19 inhibitors were combined into a common template and a series of pyridinylmethyl-substituted 1,2,5,6-tetrahydro-pyrrolo[3,2,1-*ij*]-quinolin-4-ones, **3a**−**3q**, **4a**, **4b**, **5a**, **5b**, **6a**, **6b**, **7a**, and **7b**, were synthesized. The inhibition of CYP11B2 and CYP19 was determined in comparison with fadrozole (Chart 1), which is a potent, but unselective CYP19 inhibitor showing also inhibition of 11β-hydroxylase (CYP11B1) and CYP11B2. For safety reasons, the selectivity of the new compounds against CYP11B1 and 17α-hydroxylase-17,20-lyase (CYP17), which are the crucial enzymes in the biosyntheses of glucocorticoids and androgens, respectively, were also determined.

DESIGN CONCEPT FOR DUAL INHIBITORS

All cytochrome P450s are cysteinato-heme enzymes, and the iron in the protoporphyrine acts as the reactive center to activate oxygen, which is required for the oxidation of the substrates. Therefore, competitive inhibition via coordination of this Fe by sp^2 hybrid nitrogens is a common mechanism for CYP enzyme inhibitors. First identified for CYP19 inhibitors,[18a] it was subsequently applied for inhibitors of CYP17,[19] CYP11B1,[20] and CYP11B2.[21] Despite a poor sequence identity of less than 20% across the whole CYP superfamily, CYP proteins share similar folding configurations and conserve substrate binding pockets. This makes it difficult to achieve selectivity but could be advantageous to develop dual inhibitors. In this study, a simple design strategy was applied: the combination of important structural features of selective CYP19 and CYP11B2 inhibitors into one molecule. Plenty of CYP19 inhibitors[18] have been designed and synthesized with letrozole and vorozole (Chart 1) as the most prominent representatives. It is obvious that three common structural features can be found in these two compounds: a triazole providing the sp^2 hybrid N, a methylene linker between the N-containing heterocycle and hydrophobic core, and two hydrophobic aryls. Both compounds showed potent inhibition of CYP19 and no inhibition of CYP11B2. In contrast, fadrozole (Chart 1), in which one aryl was replaced by alkyl fused onto the imidazole, was not selective toward CYP11B1 and CYP11B2 (IC_{50} of 6.3 and 0.8 nM, respectively). Hence, the scaffold of arylmethyl-substituted N-containing heterocycle was considered to be crucial for a strong CYP19 inhibition, whereas the substituents on the methylene bridge could be important for the inhibition of CYP11B enzymes. Based on this scaffold, introduction of structural features from CYP11B2 inhibitors as aryl and N-containing heterocycle as well as suitable substituents onto the methylene bridge could acquire the desired inhibition of CYP11B2 and selectivity over CYP11B1. To achieve this selectivity is challenging because the homology between CYP11B2 and CYP11B1 is as high as 93%. Our efforts to develop potent and selective CYP11B2[21] and CYP11B1[20] inhibitors had successfully led to the reference compounds **ref 1**[21h] and **ref 2**[20d] (IC_{50}(CYP11B2) of 1.1 and 24 nM, respectively) with 1,2,5,6-tetrahydro-pyrrolo[3,2,1-*ij*]quinolin-4-one as hydrophobic core. This core was considered to be important for a strong CYP11B2 inhibition and thus introduced into the scaffold to replace the original aryl. Moreover, reference compound **ref 2** was actually an even stronger inhibitor of CYP11B1 (IC_{50}(CYP11B1) = 2.2 nM), which is rendered by the imidazole moiety and cyclopropyl on the methylene bridge. According to our experience that pyridyl can cast different selectivity profiles from imdazole among CYP enzymes,[19d] pyridyl adopted from reference compounds **ref 1** was exploited as N-containing heterocycle to improve selectivity over CYP11B1. Since groups on the methylene bridge also influenced the inhibitory profiles significantly, various substituents were furnished, leading to a series of pyridinylmethyl-substituted 1,2,5,6-tetrahydro-pyrrolo[3,2,1-*ij*]quinolin-4-ones (Chart 1). When choosing substituents, three features were taken into consideration, bulkiness and electrostastic and H-bond forming properties.

dx.doi.org/10.1021/jm301408t | J. Med. Chem. 2013, 56, 460−470

Scheme 1[a]

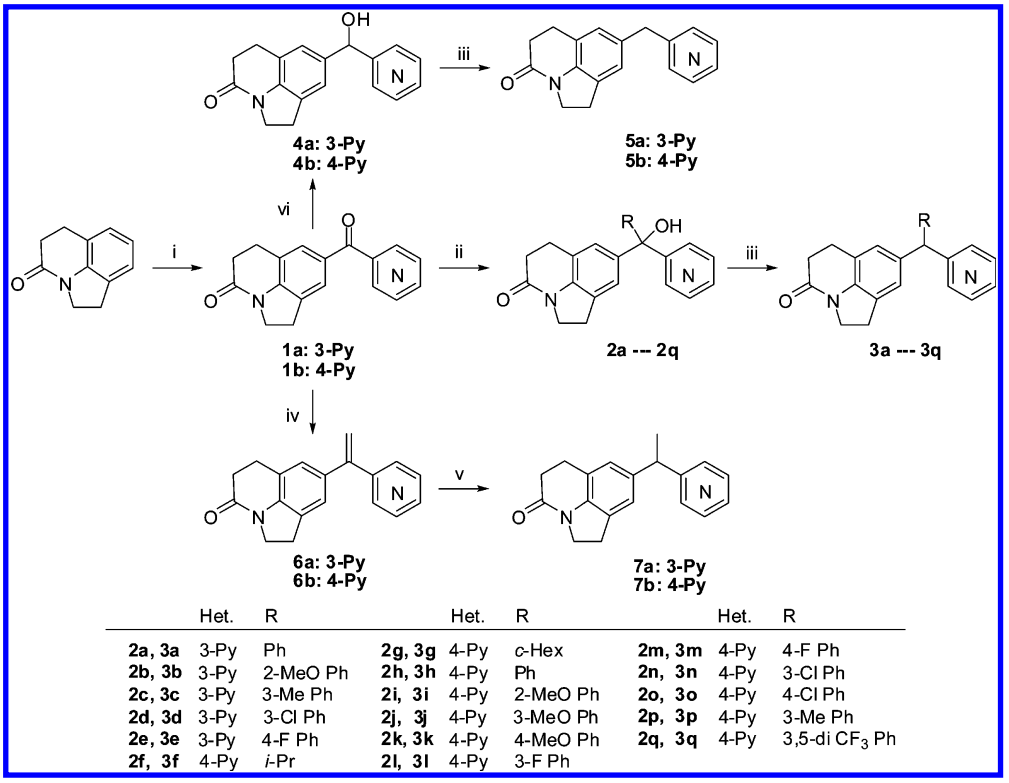

	Het.	R		Het.	R		Het.	R
2a, 3a	3-Py	Ph	**2g, 3g**	4-Py	*c*-Hex	**2m, 3m**	4-Py	4-F Ph
2b, 3b	3-Py	2-MeO Ph	**2h, 3h**	4-Py	Ph	**2n, 3n**	4-Py	3-Cl Ph
2c, 3c	3-Py	3-Me Ph	**2i, 3i**	4-Py	2-MeO Ph	**2o, 3o**	4-Py	4-Cl Ph
2d, 3d	3-Py	3-Cl Ph	**2j, 3j**	4-Py	3-MeO Ph	**2p, 3p**	4-Py	3-Me Ph
2e, 3e	3-Py	4-F Ph	**2k, 3k**	4-Py	4-MeO Ph	**2q, 3q**	4-Py	3,5-di CF_3 Ph
2f, 3f	4-Py	*i*-Pr	**2l, 3l**	4-Py	3-F Ph			

[a]Reagents and conditions: (i) Nicotinoyl or isonicotinoyl chloride hydrochloride, $AlCl_3$, 140 °C; (ii) method A, RMgX, THF, −78 °C to room temp; (iii) method B, Et_3SiH, TFA, CF_3SO_3H, CH_2Cl_2, 0 °C to room temp; (iv) CH_3PPh_3Br, *n*-BuLi, THF, −78 °C to room temp; (v) Pd/C, H_2, MeOH, room temp; (vi) $NaBH_4$, MeOH, 0 °C.

Table 1. Inhibition of CYP19, CYP11B2, CYP11B1, and CYP17 by 3-Pyridyl Compounds 4a−7a and 3a−3e

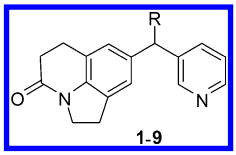

		IC_{50},[a] nM	IC_{50},[a] nM			%Inhib[b]
compd	R	CYP19[c]	CYP11B2[d]	CYP11B1[e]	SF[f]	CYP17[g]
4a	OH	>5000	>5000	750	<0.1	*i*
5a	H	3340	74	16	0.2	<3
6a	$=CH_2$	>5000	468	41	0.1	<3
7a	Me	>5000	37	4	0.1	<3
3a	Ph	2130	132	68	0.5	*i*
3b	2-MeOPh	3660	>5000	2270	<0.3	*i*
3c	3-MePh	>5000	>5000	1220	<0.2	*i*
3d	3-ClPh	1350	>5000	36	<0.1	*i*
3e	4-FPh	140	587	78	0.1	*i*
ref 1		18%[h]	1.1	715	650	6
ref 2		228	24	2.2	0.1	41
fadrozole		41	0.8	6.3	7.9	<3
letrozole		36	1420	2620	1.8	7

[a]Mean value of at least three experiments, relative standard deviation less than 25%. [b]Mean value of at least two experiments, standard deviation less than 10%; inhibitor concentration, 500 nM. [c]Human placental CYP19; substrate androstenedione, 500 nM; inhibitor concentration, 500 nM. [d]Hamster fibroblasts expressing human CYP11B2; substrate deoxycorticosterone, 100 nM. [e]Hamster fibroblasts expressing human CYP11B1; substrate deoxycorticosterone, 100 nM. [f]SF = IC_{50}(CYP11B1)/IC_{50}(CYP11B2). [g]*Escherichia coli* expressing human CYP17; substrate progesterone, 25 μM; inhibitor concentration, 2.0 μM; ketoconazole, IC_{50} = 3.5 μM. [h]Inhibitor concentration 500 nM. [i]Not determined.

RESULTS AND DISCUSSION

Chemistry. The preparation of compounds **3a−3q**, **4a**, **4b**, **5a**, **5b**, **6a**, **6b**, **7a**, and **7b** is illustrated in Scheme 1. The 1,2,5,6-tetrahydro-pyrrolo[3,2,1-*ij*]quinolin-4-one core synthesized according to previous reports[20d,21h] was converted into the pyridinyl ketones **1a** (3-py) and **1b** (4-py) via Friedel−Crafts

dx.doi.org/10.1021/jm301408t | *J. Med. Chem.* 2013, 56, 460−470

Table 2. Inhibition of CYP19, CYP11B2, CYP11B1, and CYP17 by 4-Pyridyl Compounds 2h, 4b−7b, and 3f−3q

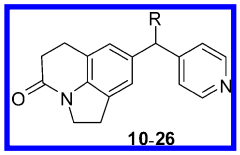

		IC_{50},[a] nM	IC_{50},[a] nM			%Inhib[b]
compd	R	CYP19[c]	CYP11B2[d]	CYP11B1[e]	SF[f]	CYP17[g]
4b	OH	>5000	563	347	0.6	<3
5b	H	2130	204	224	1.1	8
6b	$=CH_2$	565	96	1230	13	17
7b	Me	1500	74	140	1.9	*i*
3f	*i*-Pr	889	750	1420	1.9	*i*
3g	*c*-Hex	74	1290	>5000	>4	*i*
2h	Ph	105	85	745	8.8	43
3h	Ph, OH	880	390	5399	14	*i*
3i	2-MeOPh	81	128	276	2.2	33
3j	3-MeOPh	59	139	2539	18	50
3k	4-MeOPh	124	52	810	16	53
(+)-**3k**	4-MeOPh	273	46	1688	37	*i*
(−)-**3k**	4-MeOPh	92	74	511	6.9	*i*
3l	3-FPh	74	88	532	6.0	*i*
3m	4-FPh	116	56	88	1.6	55
3n	3-ClPh	19	51	646	13	58
3o	4-ClPh	55	32	92	2.9	60
3p	3-CH_3Ph	32	41	1336	33	46
3q	3,5-diCF_3Ph	246	1580	>5000	>3	*i*
ref 1		18%[h]	1.1	715	650	6
ref 2		228	24	2.2	0.1	41
fadrozole		41	0.8	6.3	7.9	<3
letrozole		36	1420	2620	1.8	7

[a]Mean value of at least three experiments, relative standard deviation less than 25%. [b]Mean value of at least two experiments, standard deviation less than 10%; inhibitor concentration, 500 nM. [c]Human placental CYP19; substrate androstenedione, 500 nM; inhibitor concentration, 500 nM. [d]Hamster fibroblasts expressing human CYP11B2; substrate deoxycorticosterone, 100 nM. [e]Hamster fibroblasts expressing human CYP11B1; substrate deoxycorticosterone, 100 nM. [f]SF = IC_{50}(CYP11B1)/IC_{50}(CYP11B2). [g]*E. coli* expressing human CYP17; substrate progesterone, 25 μM; inhibitor concentration, 2.0 μM; ketoconazole, IC_{50} = 3.5 μM. [h]Inhibitor concentration 500 nM. [i]Not determined.

acylation with the corresponding nicotinoyl or isonicotinoyl chlorides in the solid phase reactions. The ketones were transformed into alcohols **2a−2q** with various Grignard reagents. After the removal of OH groups using triethylsilane under acidic conditions, compounds **3a−3q** with various substituents at the methylene bridge were obtained. Reduction of the ketones by sodium borohydride followed by triethylsilane treatment led to nonsubstituted analogues **5a** and **5b**. The methylidene group was introduced onto the methylene bridge via Wittig reaction leading to compounds **6a** and **6b**, which were subsequently saturated by hydrogenation to yield **7a** and **7b.**

Biology. *Inhibition of Human CYP19, CYP11B2, and CYP11B1.* The synthesized compounds were investigated for their inhibitory activities against CYP19, using microsomal placenta preparations,[22a] as well as against CYP11B1 and CYP11B2, using V79 MZh cells expressing the corresponding enzymes.[22b,c] IC_{50} values are presented in comparison to reference compounds fadrozole and letrozol.

The 3-pyridyl compounds **4a**, **5a**, **6a**, **7a**, and **3a−3d** showed weak to no inhibition of CYP19 regardless of the substituents at the methylene bridge (Table 1). An exception was compound **3e** with 4-F Ph at the methylene bridge exhibiting potent inhibition with an IC_{50} value of 140 nM. In contrast, some compounds were much more potent toward CYP11B2, namely, compounds with no (**5a**) or methyl (**7a**) substituents on the methylene bridge, with IC_{50} values of 74 and 37 nM, respectively. Introduction of an unsaturated methylidene group (**6a**) decreased the inhibitory activity to 468 nM, probably due to the reduction of conformational flexibility. The loss of potency rendered by OH (**4a**) leads to the assumption that hydrophilicity is not tolerated in this area. Moreover, an interesting SAR was observed for compounds **3a−3e**. When substituted with a phenyl (**3a**), the compound was potent (IC_{50} = 132 nM). However, further introduction of methoxyl (**3b**), methyl (**3c**), and chloro (**3d**) substituents into the phenyl led to a total loss of inhibitory potency (IC_{50} > 5000 nM). Because the reduction of activity was less pronounced with the small fluorine substituent (**3e**, IC_{50} = 587 nM), it can be assumed that these effects are caused by steric restrictions. Interestingly, all the 3-pyridyl analogues showed preference for CYP11B1 with selectivity factors (SF = IC_{50}(CYP11B1)/IC_{50}(CYP11B2)) less than 0.1.

As for 4-pyridyl analogues, much more potent inhibitors of CYP19 and CYP11B2 were obtained (Table 2). When alkyl groups were introduced onto the methylene bridge, completely oppositional SARs were observed for the inhibition of CYP19 and CYP11B2. As the bulkiness of the substituents increased from H (**5b**) to methyl (**7b**), isopropyl (**3f**), and cyclohexyl (**3g**), the inhibitory potency toward CYP19 increased from 2130 to 1500, 889, and 74 nM, while a reduction of CYP11B2 inhibition from 204 (**5b**, H) to 1290 nM (**3g**, cyclohexyl) was observed. Although potent inhibitors for CYP19 or CYP11B2 were identified,

dx.doi.org/10.1021/jm301408t | J. Med. Chem. 2013, 56, 460−470

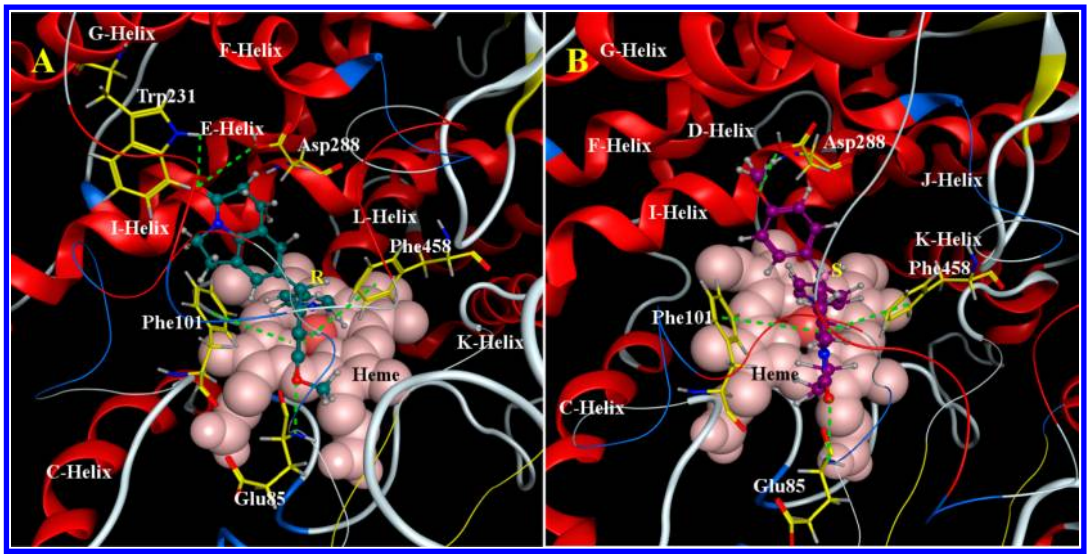

Figure 1. The binding of (A) *R*- and (B) *S*-enantiomers of **3k** in CYP11B2 homology model.

respectively, no potent dual inhibitor could be identified. Moreover, these compounds exhibited no or little selectivity over CYP11B1 with SFs ranging from 1 to 4 with the exception of the methylidene compound **6b** (SF = 13). This compound also exhibited a strong inhibition of CYP11B2 (IC_{50} = 96 nM) and a moderate inhibition of CYP19 (IC_{50} = 565 nM). Similarly, as observed in the 3-pyridinyl class, OH on the methylene bridge (**4b**) significantly decreased the inhibition for both enzymes.

In contrast, introduction of substituted phenyl moieties resulted in strong inhibition of CYP19 with IC_{50} values between 19 and 124 nM. Interestingly, the phenyl group also rendered potent CYP11B2 inhibition with IC_{50} values ranging from 32 to 139 nM. This is in contrast to the low inhibition of analogues with bulky alkyl groups, such as isopropyl (**3f**, IC_{50} = 750 nM) and cyclohexyl (**3g**, IC_{50} = 1290 nM). This finding indicates that the hydrophobic pocket in CYP11B2 might be rather flat so that the isopropyl or cyclohexyl group does not fit in well. Possible $\pi-\pi$ interactions between phenyl and some amino acid residues in the pocket might also be responsible for this difference. Opposing effects on the inhibition of CYP19 and CYP11B2 were observed for the H-bond acceptors (OMe and F) on the phenyl ring. Regarding CYP19, the 2- and 3-methoxy-substituted compounds, **3i** and **3j**, showed increased inhibition compared with the nonsubstituted **2h** (IC_{50} = 105 nM) with IC_{50} values of 81 and 59 nM, respectively, whereas the 4-MeO analogue **3k** exhibited a slightly decreased inhibition (IC_{50} = 124 nM). In contrast, compounds **3i** and **3j** showed a reduced inhibition of CYP11B2 (IC_{50} values around 130 nM) compared with **2h** (IC_{50} = 85 nM), while compound **3k** was more potent (IC_{50} = 52 nM). Similar observations were also found for the F analogues **3l** and **3m**. Nonetheless, a chloro (**3n** and **3o**) and methyl (**3p**) substitution on the phenyl moiety increased the inhibitory potency toward both enzymes regardless of the substitution positions, leading to potent dual inhibitors (IC_{50} values below 50 nM for both enzymes). Although 4-ClPh-substituted compound **3o** exhibited poor selectivity (SF = 2.9) similar to 4-FPh analogue **3m** (SF = 1.6) toward CYP11B1, compounds **3n** (3-ClPh) and **3p** (3-CH_3Ph) showed good selectivity with SFs of 13 and 33, respectively. Especially compound **3p** turned out to be superior to the reference compounds fadrozle and letrozole considering the inhibitory potency toward CYP19 and CYP11B2, as well as the selectivity regarding CYP11B1. It is interesting to observe that the compounds with the 3-substituted Ph moiety were more selective than the corresponding 4-substituted Ph analogues (for comparison, **3j** and **3k**, **3l** and **3m**, and **3n** and **3o**). Also, 3-substituted Ph compounds were more potent toward CYP19, whereas 4-substituted Ph derivatives inhibited CYP11B2 in a stronger way. Furthermore, the loss of CYP11B2 inhibition for compound **3q**, which was substituted with two trifluoromethyl groups in the *m*-position, indicated that the binding pocket is very narrow.

The potent (IC_{50}(CYP19) = 124 nM and IC_{50}(CYP11B2) = 52 nM) and selective (SF = 16) dual inhibitor **3k** was resolved into pure enantiomers to examine the influence of the chiral center on biological activity. One enantiomer, (+)-**3k**, showed similar CYP11B2 inhibition (IC_{50} = 46 vs 52 nM) and enhanced selectivity (SF = 37 vs 16); however, the CYP19 inhibitory activity was reduced (IC_{50} = 273 vs 124 nM). Contrarily, the other enantiomer, (−)-**3k**, exhibited a little stronger inhibition of CYP19 (IC_{50} = 92 vs 124 nM); but CYP11B2 inhibition (IC_{50} = 74 vs 52 nM) and selectivity (SF = 7 vs 16) were decreased. Since the aim is to obtain potent and selective dual inhibition, the racemate is considered to be advantageous. The modest potency difference between enantiomers toward CYP19 and minor difference toward CYP11B2 indicate that the binding sites of both enzymes are relatively promiscuous, which is supported by the docking results.

Selectivity over Human CYP17. The inhibition of CYP17 by the synthesized compounds was evaluated due to its important role in the biosynthesis of androgens. The percent inhibition values were obtained using the 90000*g* sediment of *E. coli* coexpressing human CYP17 and cytochrome P450 reductase at an inhibitor concentration of 2 μM.[22d,e] The potent dual inhibitors **2h** and **3i**−**3p** showed weak inhibition (around 50% at 2 μM) toward CYP17, which is tolerable considering their strong potency against CYP19 and CYP11B2 with IC_{50} values ranging from 19 to 139 nM.

Docking Studies. For better understanding of the binding of these dual inhibitors into their target enzymes, especially the tolerance of both enantiomers, the *R*- and *S*-enantiomers of **3k** were docked into the CYP19 crystal (PDB ID 3EQM) and CYP11B2 homology model.[21b] Since the active site in CYP19 was relatively capacious to accommodate both enantiomers, the three aromatic moieties, that is, tetrahydropyrroloquinolinone,

dx.doi.org/10.1021/jm301408t | *J. Med. Chem.* 2013, 56, 460−470

phenyl, and pyridyl occupied the same pockets with only minor shift in position if comparing both enantiomers (Figure S1, see Supporting Information). As for CYP11B2, when *R*-enantiomer fit into the binding pocket, the pyridyl group coordinated to the heme iron with its sp^2 hybrid N in a nearly perpendicular manner (Figure 1A). It also bolstered the other two aromatic rings which twisted into an "L" shape and were spatially plumb to each other. The tetrahydropyrroloquinolinone moiety leaned on I-helix and oriented to the N-terminus of I-helix; while the phenyl group directed to B−B′ loop. The *S*-enantiomer presented a similar binding mode except that the tetrahydropyrroloquinolinone and phenyl moieties exchanged their locations (Figure 1B). Since these enantiomers were more potent toward CYP11B2 with less difference in inhibitory potency, the binding of CYP11B2 was further analyzed. Scrutinizing the binding pocket revealed that two amino acid residues Tyr456 and Leu198 delimiting the boundary obstructed the aromatic rings that leaned on I-helix from orientating toward the C-terminus of I-helix (Figure 2C).

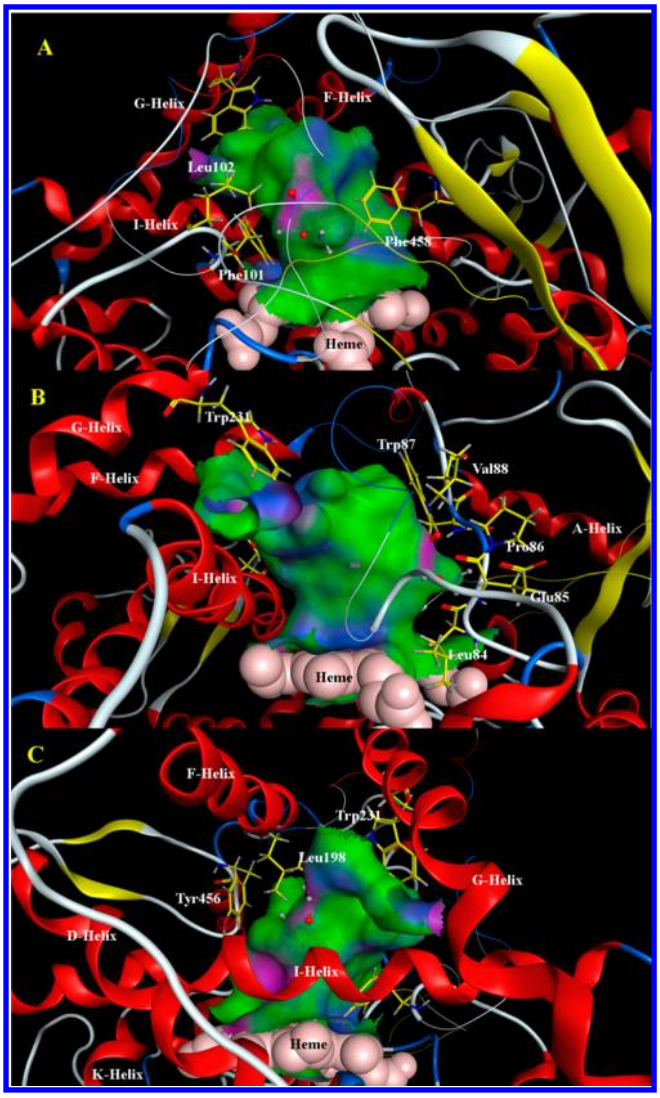

Figure 2. The confines of the binding pocket in CYP11B2. (A) the narrow planar cleft near B−B′ loop (view facing I-helix); (B) the bottom of the cleft (side view); (C) obstruction in the C-terminal direction of I-helix (view facing B−B′ loop).

This obstruction forced both enantiomers to adopt consentaneous binding modes with the interchange of two aromatic ring positions as the only major difference. Moreover, Trp231, the ceiling of this region, and Asp288 can form hydrogen bonds with the carbonyl of tetrahydropyrroloquinolinone or methoxyl on the phenyl group (Figure 1). Furthermore, the aromatic rings pointing to the B−B′ loop actually wedged in a narrow planar cleft confined by Phe101, Leu102, and Phe458 (Figure 2A). These two phenylalanines formed $\pi-\pi$ interactions with the aromatic rings in parallel or perpendicular manners, respectively (Figure 1). The narrow planar feature of the pocket and the possible $\pi-\pi$ interactions are the reasons why the inhibitory potency dove along with the increase of substituent bulkiness when alkyl groups were furnished on the methylene bridge, whereas phenyl rendered a much more potent inhibition although it was bulky as well. This pocket was also rather shallow with the bottom defined by amino acid residues on the B−B′ loop such as Val88, Trp87, Pro86, Glu85, and Leu84 (Figure 2B). Among them, the backbones of Glu85 and Pro86 were accessible and therefore could form hydrogen bonds with carbonyl, MeO, F, or OH on the corresponding aromatic rings, especially the ones at *para*-position (Figure 1). This could also be one of the factors responsible for the 4-substituted phenyl analogues being more potent than 3- or 2-substituted ones toward CYP11B2.

CONCLUSION

Estrogen deficiency has been observed to be closely correlated with CVD, which was mediated to a large extent by abnormally high concentrations of aldosterone. The application of CYP19 inhibitors to postmenopausal BC patients reduces estrogens to undetectable levels in plasma. However, this therapy also increases the risk of CVD strongly. Accordingly, the rationale to develop dual inhibitors of CYP19 and CYP11B2 for an improved BC therapy is obvious. With such dual inhibitors as adjuvant therapy, the overall survival and life quality of BC patients would be further improved.

By combining the 1,2,5,6-tetrahydro-pyrrolo[3,2,1-*ij*]-quinolin-4-one core from CYP11B2 inhibitors with structural elements derived from CYP19 inhibitors, a series of potent dual inhibitors were designed and synthesized. The substituents on the methylene bridge showed significant influence on the inhibitory activity in the 4-pyridyl series. Opposite SARs were commonly observed that modifications increasing the inhibition of one enzyme always reduced that of the other. The compromise of these conflicts finally led to compounds **3j**, **3l**, **3n**, and **3p** as potent and selective dual inhibitors of CYP19 and CYP11B2. These inhibition profiles together with reasonable selectivity toward CYP17 and CYP11B1 make these compounds ideal candidates for further evaluation *in vivo* and the proof of concept, especially compound **3p**, which exhibited IC_{50} values of 32 and 41 nM for CYP19 and CYP11B2, respectively, and a SF of 33 over CYP11B1.

Since three series of substituted methylene tetrahydropyrroloquinolinones, which differed predominantly in N-containing heterocycles (i.e., 1-imidazoles,[20d] 3- and 4-pyridines), have been designed, synthesized, and tested as CYP enzyme inhibitors, their inhibition profiles among these enzymes were compared and analyzed as shown in Table 3. It is apparent that all compounds showed no inhibition toward CYP17, while for the other three enzymes, situations were complicated but also interesting. When the alkyl groups were substituted at the methylene bridge, 1-Im and 3-Py compounds exhibited weak to no inhibition toward CYP19, whereas very potent inhibition of CYP11Bs. Since the inhibition of CYP11B1 is always stronger than that of CYP11B2, selective CYP11B1 inhibitors were thus identified. As for 4-Py

dx.doi.org/10.1021/jm301408t | *J. Med. Chem.* 2013, 56, 460−470

Table 3. Inhibitory Tendency of N-Heterocycle Substituted Methylene Tetrahydropyrroloquinolinones[a]

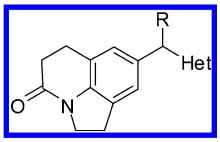

Het =	1-Im[b]		3-Py		4-Py	
R =	alkyl	subst. Ph	alkyl[c]	subst. Ph[d]	alkyl[e]	subst. Ph
CYP19	W	VP	N	W or P	N to VP	VP
CYP11B2	VP	VP	VP	N or M	VP to N	VP
CYP11B1	EP	VP	EP	VP or N	P to N	W
CYP17	N	N	N	N	N	N

[a]Only general trends were considered, outliers were not mentioned. N no inhibition, IC_{50} >1000 nM; W indicates weak inhibition, 1000 nM ≥ IC_{50} >500 nM; M indicates moderate inhibition, 500 nM ≥ IC_{50} >250 nM; P indicates potent inhibition, 250 nM ≥ IC_{50} >100 nM; VP indicates very potent inhibition, 100 nM ≥ IC_{50} > 20 nM; EP indicates extremely potent inhibition, 20 nM ≥ IC_{50}. [b]Data adopted from ref 20d. [c]Number of examples is limited. [d]inhibition varied dramatically to subtle differences in structure, extremely sensitive to alternation of substituents. [e]Inhibition is sensitive to the bulkiness of alkyls and ranges very widely. Trends along the bulkiness elevation are presented in the table.

with an alkyl substitution, the inhibition of all three enzymes altered gradually according to the bulkiness of the alkyl, ranging from no inhibition to high potency. As discussed above, the effects rendered by a given modification on the inhibition of CYP11Bs are usually opposite to those on CYP19 inhibition. In contrast, compounds with substituted phenyl at the methylene bridge acted in different manners. 1-Im analogues showed very potent inhibition of all CYP enzymes except CYP17; while 4-Py compounds are very potent inhibitors of CYP19 and CYP11B2. The inhibitory profiles of 3-Py compounds are extremely sensitive to the subtle alternation of the substituents on phenyl moiety, dramatic deviations of inhibition are therefore observed for CYP19, CYP11B1, and CYP11B2. Consistent with our previous findings,[19d] 1-Im and 3- or 4-Py rendered distinct inhibition profiles among steroidogenic CYP enzymes, which could be the results of differences in size, interaction angle, and electron density on the sp^2 hybrid N.

EXPERIMENTAL SECTION

Biology. *CYP19 Preparation and Assay.* Human CYP19 was obtained from microsomal preparations of human placenta, and the assay was performed using the ^3H_2O-method as described and [1β-^{3}H]androstenedione as substrate.[22a]

Inhibition of CYP11B1 and CYP11B2. V79MZh cells expressing human CYP11B1 or CYP11B2 were incubated with [1,2-^{3}H]-11-deoxycorticosterone as substrate and the inhibitor at different concentrations. The assay was performed as previously described.[22b,c]

CYP17 Preparation and Assay. The inhibition of CYP17 was determined using the 90000*g* sediment of *E. coli* coexpressing human CYP17 and cytochrome P450 reductase[22d] with progesterone as substrate and NADPH as cofactor.[22e]

Chemistry. *General Method.* Melting points were determined on a Mettler FP1 melting point apparatus and are uncorrected. ^{1}H NMR and ^{13}C NMR spectra were measured on a Bruker DRX-500 (500 MHz). Chemical shifts are given in parts per million (ppm), and TMS was used as an internal standard for spectra obtained. All coupling constants (*J*) are given in Hz. ESI (electrospray ionization) mass spectra were determined on a TSQ quantum (Thermo Electron Corporation) instrument. The purities of the final compounds were controlled by Surveyor-LC-system. Purities were greater than 95%. Column chromatography was performed using silica-gel 60 (50−200 μm), and reaction progress was determined by TLC analysis on Alugram SIL G/UV_{254} (Macherey-Nagel). Reagents and solvents were used as obtained from commercial suppliers without further purification.

Resolution of Racemate. Enantiomers were separated via preparative HPLC on a Agilent Technologies 1200 series system (quaternary pump, MWD, fraction collector) using a NucleoCel Delta column, 0.8 cm × 25 cm. Retention times (t_R) were determined with an analytical column using 0.3 mL/min and UV detection (254 nm). The ee values were measured on a Merck-Hitachi LaChrome D-7000 System (isocratic pump L7100, diode array detector L7455, autosampler L-7200) using a Chiracel OD-H column, 0.46 cm ×25 cm.

*8-(Pyridin-3-ylcarbonyl)-1,2,5,6-tetrahydro-4H-pyrrolo[3,2,1-ij]-quinolin-4-one (**1a**).* Starting materials 1,2,5,6-tetrahydro-4*H*-pyrrolo-[3,2,1-*ij*]quinolin-4-one (0.50 g, 2.89 mmol), nicotinoyl chloride hydrochloride (0.77 g, 4.33 mmol), and $AlCl_3$ (2.60 g,19.5 mmol) were melted at 140 °C for 4 h followed by being cooled to 0 °C. A mixture of ice/water was added to decompose the excessive $AlCl_3$, and the resulting mixture was stirred at ambient temperature for 1 h. Extraction with $CHCl_3$ (3 × 20 mL) gave the organic layers, which were combined and dried over $MgSO_4$. After removal of solvent in vacuo, the residue was purified by flash chromatography column on silica gel (methanol/dichloromethane, 1/100, R_f = 0.07) to give yellow solids (0.69 g, 86%), mp 135−137 °C. ^{1}H NMR (500 MHz, $CDCl_3$): δ 2.72 (t, *J* = 7.8 Hz, 2H), 3.03 (t, *J* = 7.8 Hz, 2H), 3.25 (t, *J* = 8.5 Hz, 2H), 4.16 (t, *J* = 8.5 Hz, 2H), 7.45 (ddd, *J* = 0.8, 4.9, 7.9 Hz, 1H), 7.54 (s, 1H), 7.59 (s, 1H), 8.08 (dt, *J* = 2.0, 7.9 Hz, 1H), 8.80 (dd, *J* = 1.7, 4.7 Hz, 1H), 8.94 (dd, *J* = 0.8, 2.2 Hz, 1H). MS (ESI) *m*/*z* = 279 [M + H]$^+$.

*8-(Pyridin-4-ylcarbonyl)-1,2,5,6-tetrahydro-4H-pyrrolo[3,2,1-ij]-quinolin-4-one (**1b**).* Starting materials 1,2,5,6-tetrahydro-4*H*-pyrrolo-[3,2,1-*ij*]quinolin-4-one (1.00 g, 5.77 mmol), isonicotinoyl chloride hydrochloride (1.54 g, 8.65 mmol), and $AlCl_3$ (3.85 g, 28.9 mmol) were melted at 140 °C for 4 h followed by being cooled to 0 °C. A mixture of ice/water was added to decompose the excessive $AlCl_3$, and the resulting mixture was stirred at ambient temperature for 1 h. Extraction with $CHCl_3$ (3 × 20 mL) gave the organic layers, which were combined and dried over $MgSO_4$. After removal of solvent in vacuo, the residue was purified by flash chromatography column on silica gel (methanol/dichloromethane, 1/100, R_f = 0.05) to give yellow solids (1.15 g, 72%), mp 171−173 °C. ^{1}H NMR (500 MHz, $CDCl_3$): δ 2.74 (t, *J* = 7.8 Hz, 2H), 3.03 (t, *J* = 7.9 Hz, 2H), 3.24 (t, *J* = 8.5 Hz, 2H), 4.16 (t, *J* = 8.5 Hz, 2H), 7.52 (dd, *J* = 1.6, 4.4 Hz, 2H), 7.53 (s, 1H), 7.58 (s, 1H), 8.80 (dd, *J* = 1.6, 4.4 Hz, 2H). MS (ESI) *m*/*z* = 279 [M + H]$^+$.

Method A: Grignard Reaction. To a solution of a ketone (1.0 equiv) in anhydrous THF was added dropwise a solution of an appropriate Grignard reagent (2.0−3.0 equiv) under an atmosphere of nitrogen at −78 °C. The reaction was stirred at the same temperature for another 1 h, and subsequently warmed to room temperature. After being stirred for 15 h, the reaction was quenched with saturated aqueous $NHCl_4$ (5 mL), extracted with ethyl acetate (3 × 10 mL), dried over $MgSO_4$, and concentrated in vacuo. The residue was purified by flash chromatography on silica gel (methanol/dichloromethane, 0 to 1:30) to yield the corresponding alcohol.

*8-[Hydroxy(phenyl)pyridin-4-ylmethyl]-1,2,5,6-tetrahydro-4H-pyrrolo[3,2,1-ij]quinolin-4-one (**2h**).* The title compound was obtained according to Method A using **1b** (200 mg, 0.72 mmol) and phenylmagnesium bromide (1 M in THF, 2.16 mL, 2.16 mmol) in anhydrous THF (5 mL) as pale yellow solids (120 mg, 47%), mp 196−197 °C. ^{1}H NMR (500 MHz, $CDCl_3$): δ 2.63 (t, *J* = 7.7 Hz, 2H), 2.88 (t, *J* = 7.7 Hz, 2H), 3.11 (t, *J* = 8.3 Hz, 2H), 3.53 (s, br, 1H), 4.04 (t, *J* = 8.3 Hz, 2H), 6.88 (s, 1H), 6.93 (s, 1H), 7.25−7.33 (m, 7H), 8.49 (d, *J* = 3.2 Hz, 2H). ^{13}C NMR (125 MHz, $CDCl_3$): δ 24.4, 27.7, 31.5, 45.4, 81.2, 119.5, 122.6, 123.1, 125.3, 127.7, 127.8, 128.2, 128.7, 140.9, 141.4, 145.7, 149.4, 155.6, 167.6. MS (ESI) *m*/*z* = 357 [M + H]$^+$.

Method B: Triethylsilane Reduction. To an alcohol (1.0 equiv) in anhydrous dichloromethane was added in sequence by syringe trifluoroacetic acid (10 equiv), triethylsilane (3.0 equiv), and trifluoromethanesulfonic acid (0.1 equivalent) under an atmosphere of nitrogen at 0 °C. The resulting solution was stirred at room temperature for 18−48 h. Afterward, the reaction mixture was separated, and the queous layer was extracted with dichloromethane (2 × 10 mL). The combined organic

dx.doi.org/10.1021/jm301408t | J. Med. Chem. 2013, 56, 460−470

layers were washed with aqueous $NaHCO_3$ and brine, dried over $MgSO_4$, and concentrated in vacuo. The residue was purified by flash chromatograph on silica gel (methanol/dichloromethane, 0 to 1:40) to yield the corresponding dehydroxyl product.

*8-(Pyridin-3-ylmethyl)-1,2,5,6-tetrahydro-4H-pyrrolo[3,2,1-ij]-quinolin-4-one (**5a**).* The title compound was obtained according to Method B using **4a** (70 mg, 0.25 mmol), trifluoroacetic acid (0.19 mL, 2.50 mmol), triethylsilane (0.12 mL, 0.75 mmol), and trifluoromethanesulfonic acid (2 μL, 0.02 mmol) in anhydrous CH_2Cl_2 (5 mL) as white solids (44 mg, 67%), mp 108−110 °C. ^{1}H NMR (500 MHz, $CDCl_3$): δ 2.65 (t, *J* = 7.7 Hz, 2H), 2.92 (t, *J* = 7.7 Hz, 2H), 3.14 (t, *J* = 8.5 Hz, 2H), 3.90 (s, 2H), 4.06 (t, *J* = 8.5 Hz, 2H), 6.80 (s, 1H), 6.88 (s, 1H), 7.20 (dd, *J* = 4.8, 7.7 Hz, 1H), 8.46 (d, *J* = 7.8 Hz, 1H), 8.46 (dd, *J* = 1.1, 7.8 Hz, 1H), 8.49 (d, *J* = 1.3 Hz, 1H). MS (ESI) *m*/*z* = 265 $[M + H]^+$.

*8-[Phenyl(pyridin-3-yl)methyl]-1,2,5,6-tetrahydro-4H-pyrrolo-[3,2,1-ij]quinolin-4-one (**3a**).* The title compound was obtained according to Method B using **2a** (60 mg, 0.17 mmol), trifluoroacetic acid (0.13 mL, 1.68 mmol), triethylsilane (82 μL, 0.51 mmol), and trifluoromethanesulfonic acid (2 μL, 0.02 mmol) in anhydrous CH_2Cl_2 (3 mL) as pale yellow solids (46 mg, 81%), mp 142−144 °C. ^{1}H NMR (500 MHz, $CDCl_3$): δ 2.65 (t, *J* = 7.7 Hz, 2H), 2.89 (t, *J* = 7.7 Hz, 2H), 3.12 (t, *J* = 8.4 Hz, 2H), 4.06 (t, *J* = 8.4 Hz, 2H), 5.49 (s, 1H), 6.74 (s, 1H), 6.80 (s, 1H), 7.10 (m, 2H), 7.22 (dd, *J* = 4.7, 7.9 Hz, 1H), 7.24 (m, 1H), 7.31 (m, 2H), 7.40 (dt, *J* = 1.7, 7.9 Hz, 1H), 8.42 (d, *J* = 2.0 Hz, 1H), 8.48 (dd, *J* = 1.4, 4.7 Hz, 1H). MS (ESI) *m*/*z* = 341 $[M + H]^+$.

*8-[(2-Methoxyphenyl)(pyridin-3-yl)methyl]-1,2,5,6-tetrahydro-4H-pyrrolo[3,2,1-ij]quinolin-4-one (**3b**).* The title compound was obtained according to Method B using **2b** (57 mg, 0.15 mmol), trifluoroacetic acid (0.11 mL, 1.48 mmol), triethylsilane (71 μL, 0.44 mmol), and trifluoromethanesulfonic acid (2 μL, 0.02 mmol) in anhydrous CH_2Cl_2 (4 mL) as pale yellow solids (31 mg, 56%), mp 65−68 °C. ^{1}H NMR (500 MHz, $CDCl_3$): δ 2.65 (t, *J* = 7.7 Hz, 2H), 2.89 (t, *J* = 7.7 Hz, 2H), 3.12 (t, *J* = 8.5 Hz, 2H), 3.74 (s, 3H), 4.06 (t, *J* = 8.5 Hz, 2H), 5.85 (s, 1H), 6.71 (s, 1H), 6.78 (s, 1H), 6.84−6.91 (m, 3H), 7.20 (dd, *J* = 4.8, 7.8 Hz, 1H), 7.25 (m, 1H), 7.36 (dt, *J* = 1.7, 7.8 Hz, 1H), 8.38 (d, *J* = 2.1 Hz, 1H), 8.45 (dd, *J* = 1.5, 4.8 Hz, 1H). MS (ESI) *m*/*z* = 371 $[M + H]^+$.

*8-[(3-Methylphenyl)(pyridin-3-yl)methyl]-1,2,5,6-tetrahydro-4H-pyrrolo[3,2,1-ij]quinolin-4-one (**3c**).* The title compound was obtained according to Method B using **2c** (62 mg, 0.17 mmol), trifluoroacetic acid (0.13 mL, 1.67 mmol), triethylsilane (0.81 μL, 0.50 mmol), and trifluoromethanesulfonic acid (2 μL, 0.02 mmol) in anhydrous CH_2Cl_2 (4 mL) as pale yellow solids (30 mg, 50%), mp 164−166 °C. ^{1}H NMR (500 MHz, $CDCl_3$): δ 2.31 (s, 3H), 2.65 (t, *J* = 7.7 Hz, 2H), 2.90 (t, *J* = 7.7 Hz, 2H), 3.12 (t, *J* = 8.4 Hz, 2H), 4.06 (t, *J* = 8.4 Hz, 2H), 5.44 (s, 1H), 6.73 (s, 1H), 6.80 (s, 1H), 6.88 (d, *J* = 7.6 Hz, 1H), 6.92 (s, 1H), 7.06 (d, *J* = 7.5 Hz, 1H), 7.18−7.23 (m, 2H), 7.40 (dd, *J* = 1.8, 7.9 Hz, 1H), 8.41 (d, *J* = 1.6 Hz, 1H), 8.47 (dd, *J* = 1.2, 4.7 Hz, 1H). MS (ESI) *m*/*z* = 355 $[M + H]^+$.

*8-[(3-Chlorophenyl)(pyridin-4-yl)methyl]-1,2,5,6-tetrahydro-4H-pyrrolo[3,2,1-ij]quinolin-4-one (**3d**).* The title compound was obtained according to Method B using **2d** (72 mg, 0.18 mmol), trifluoroacetic acid (0.14 mL, 1.84 mmol), triethylsilane (0.89 μL, 0.55 mmol), and trifluoromethanesulfonic acid (2 μL, 0.02 mmol) in anhydrous CH_2Cl_2 (4 mL) as to give pale yellow solids (36 mg, 53%), mp 129−131 °C. ^{1}H NMR (500 MHz, $CDCl_3$): δ 2.68 (t, *J* = 7.7 Hz, 2H), 2.93 (t, *J* = 7.7 Hz, 2H), 3.16 (t, *J* = 8.4 Hz, 2H), 4.10 (t, *J* = 8.4 Hz, 2H), 5.48 (s, 1H), 6.73 (s, 1H), 6.80 (s, 1H), 7.01 (m, 1H), 7.10 (s, 1H), 7.27 (m, 3H), 7.41 (d, *J* = 7.9 Hz, 1H), 8.43 (d, *J* = 1.9 Hz, 1H), 8.52 (dd, *J* = 1.3, 4.7 Hz, 1H). MS (ESI) *m*/*z* = 375 $[M + H]^+$.

*8-[(4-Fluorophenyl)(pyridin-3-yl)methyl]-1,2,5,6-tetrahydro-4H-pyrrolo[3,2,1-ij]quinolin-4-one (**3e**).* The title compound was obtained according to Method B using **2e** (90 mg, 0.24 mmol), trifluoroacetic acid (0.18 mL, 2.40 mmol), triethylsilane (0.12 mL, 0.72 mmol), and trifluoromethanesulfonic acid (2 μL, 0.02 mmol) in anhydrous CH_2Cl_2 (5 mL) as pale yellow solids (50 mg, 58%), mp 175−177 °C. ^{1}H NMR (500 MHz, $CDCl_3$): δ 2.66 (t, *J* = 7.7 Hz, 2H), 2.90 (t, *J* = 7.7 Hz, 2H), 3.13 (t, *J* = 8.4 Hz, 2H), 4.07 (t, *J* = 8.4 Hz, 2H), 5.47 (s, 1H), 6.71 (s, 1H), 6.78 (s, 1H), 7.00 (m, 2H), 7.05 (m, 2H), 7.24 (dd, *J* = 4.8, 7.9 Hz, 1H), 7.38 (dt, *J* = 1.7, 7.9 Hz, 1H), 8.40 (d, *J* = 1.0 Hz, 1H), 8.49 (dd, *J* = 1.4, 4.7 Hz, 1H). MS (ESI) *m*/*z* = 359 $[M + H]^+$.

*8-(Pyridin-4-ylmethyl)-1,2,5,6-tetrahydro-4H-pyrrolo[3,2,1-ij]-quinolin-4-one (**5b**).* The title compound was obtained according to Method B using **4b** (125 mg, 0.45 mmol), trifluoroacetic acid (0.34 mL, 4.46 mmol), triethylsilane (0.22 mL, 1.34 mmol), and trifluoromethanesulfonic acid (4 μL, 0.04 mmol) in anhydrous CH_2Cl_2 (5 mL) as pale yellow solids (65 mg, 55%), mp 199−200 °C. ^{1}H NMR (500 MHz, $CDCl_3$): δ 2.66 (t, *J* = 7.7 Hz, 2H), 2.93 (t, *J* = 7.7 Hz, 2H), 3.15 (t, *J* = 8.5 Hz, 2H), 3.89 (s, 2H), 4.07 (t, *J* = 8.5 Hz, 2H), 6.80 (s, 1H), 6.88 (s, 1H), 7.09 (dd, *J* = 1.4, 4.5 Hz, 2H), 8.50 (dd, *J* = 1.4, 4.5 Hz, 2H). MS (ESI) *m*/*z* = 265 $[M + H]^+$.

*8-(2-Methyl-1-pyridin-4-ylpropyl)-1,2,5,6-tetrahydro-4H-pyrrolo-[3,2,1-ij]quinolin-4-one (**3f**).* The title compound was obtained according to Method B using **2f** (167 mg, 0.52 mmol), trifluoroacetic acid (0.40 mL, 5.18 mmol), triethylsilane (0.25 mL, 1.55 mmol), and trifluoromethanesulfonic acid (5 μL, 0.05 mmol) in anhydrous CH_2Cl_2 (8 mL) as white solids (105 mg, 66%), mp 137−139 °C. ^{1}H NMR (500 MHz, $CDCl_3$): δ 0.88 (q, *J* = 6.5 Hz, 6H), 2.40−2.47 (m, 1H), 2.64 (t, *J* = 7.7 Hz, 2H), 2.92 (t, *J* = 7.7 Hz, 2H), 3.14 (t, *J* = 8.4 Hz, 2H), 3.32 (d, *J* = 10.9 Hz, 1H), 4.04 (t, *J* = 8.4 Hz, 2H), 6.86 (s, 1H), 6.96 (s, 1H), 7.18 (dd, *J* = 1.4, 4.6 Hz, 2H), 8.47 (dd, *J* = 1.4, 4.6 Hz, 2H). MS (ESI) *m*/*z* = 307 $[M + H]^+$.

*8-[Cyclohexyl(pyridin-3-yl)methyl]-1,2,5,6-tetrahydro-4H-pyrrolo-[3,2,1-ij]quinolin-4-one (**3g**).* The title compound was obtained according to Method B using **2g** (150 mg, 0.41 mmol), trifluoroacetic acid (0.32 mL, 4.14 mmol), triethylsilane (0.20 mL, 1.24 mmol), and trifluoromethanesulfonic acid (4 μL, 0.04 mmol) in anhydrous CH_2Cl_2 (8 mL) as white crystals (80 mg, 54%), mp 83−85 °C. ^{1}H NMR (500 MHz, $CDCl_3$): δ 0.86 (m, 2H), 1.14−1.26 (m, 3H), 1.62−1.70 (m, 5H), 2.05 (m, 1H), 2.64 (t, *J* = 7.7 Hz, 2H), 2.92 (t, *J* = 7.7 Hz, 2H), 3.14 (t, *J* = 8.4 Hz, 2H), 3.40 (d, *J* = 10.9 Hz, 1H), 4.04 (t, *J* = 8.4 Hz, 2H), 6.85 (s, 1H), 6.95 (s, 1H), 7.17 (dd, *J* = 1.4, 4.6 Hz, 2H), 8.46 (dd, *J* = 1.4, 4.6 Hz, 2H). MS (ESI) *m*/*z* = 347 $[M + H]^+$.

*8-[Phenyl(pyridin-4-yl)methyl]-1,2,5,6-tetrahydro-4H-pyrrolo-[3,2,1-ij]quinolin-4-one (**3h**).* The title compound was obtained according to Method B using **2h** (70 mg, 0.20 mmol), trifluoroacetic acid (0.15 mL, 1.96 mmol), triethylsilane (95 μL, 0.59 mmol), and trifluoromethanesulfonic acid (2 μL, 0.02 mmol) in anhydrous CH_2Cl_2 (5 mL) as pale yellow solids (48 mg, 72%), mp 168−169 °C. ^{1}H NMR (500 MHz, $CDCl_3$): δ 2.66 (t, *J* = 7.7 Hz, 2H), 2.90 (t, *J* = 7.7 Hz, 2H), 3.13 (t, *J* = 8.4 Hz, 2H), 4.07 (t, *J* = 8.4 Hz, 2H), 5.43 (s, 1H), 6.73 (s, 1H), 6.79 (s, 1H), 7.04 (d, *J* = 5.3 Hz, 2H), 7.08 (d, *J* = 7.2 Hz, 2H), 7.26 (m, 1H), 7.32 (t, *J* = 7.4 Hz, 2H), 8.52 (d, *J* = 5.3 Hz, 2H). MS (ESI) *m*/*z* = 341 $[M + H]^+$.

*8-[(2-Methoxyphenyl)(pyridin-4-yl)methyl]-1,2,5,6-tetrahydro-4H-pyrrolo[3,2,1-ij]quinolin-4-one (**3i**).* The title compound was obtained according to Method B using **2i** (77 mg, 0.20 mmol), trifluoroacetic acid (0.15 mL, 1.99 mmol), triethylsilane (97 μL, 0.60 mmol), and trifluoromethanesulfonic acid (2 μL, 0.02 mmol) in anhydrous CH_2Cl_2 (4 mL) as pale yellow solids (55 mg, 75%), mp 70−72 °C. ^{1}H NMR (500 MHz, $CDCl_3$): δ 2.66 (t, *J* = 7.7 Hz, 2H), 2.90 (t, *J* = 7.7 Hz, 2H), 3.12 (t, *J* = 8.5 Hz, 2H), 3.73 (s, 3H), 4.07 (t, *J* = 8.5 Hz, 2H), 5.80 (s, 1H), 6.71 (s, 1H), 6.78 (s, 1H), 6.83 (m, 1H), 6.90 (m, 2H), 7.00 (d, *J* = 4.6 Hz, 2H), 7.26 (m, 1H), 8.48 (d, *J* = 4.6 Hz, 2H). MS (ESI) *m*/*z* = 371 $[M + H]^+$.

*8-[(3-Methoxyphenyl)(pyridin-4-yl)methyl]-1,2,5,6-tetrahydro-4H-pyrrolo[3,2,1-ij]quinolin-4-one (**3j**).* The title compound was obtained according to Method B using **2j** (102 mg, 0.26 mmol), trifluoroacetic acid (0.20 mL, 2.64 mmol), triethylsilane (0.13 mL, 0.79 mmol), and trifluoromethanesulfonic acid (2 μL, 0.03 mmol) in anhydrous CH_2Cl_2 (8 mL) as pale yellow solids (48 mg, 50%), mp 148−150 °C. ^{1}H NMR (500 MHz, $CDCl_3$): δ 2.66 (t, *J* = 7.7 Hz, 2H), 2.90 (t, *J* = 7.7 Hz, 2H), 3.12 (t, *J* = 8.4 Hz, 2H), 4.06 (t, *J* = 8.4 Hz, 2H), 5.39 (s, 1H), 6.63 (m, 1H), 6.68 (d, *J* = 7.7 Hz, 1H), 6.72 (s, 1H), 6.80 (m, 2H), 7.04 (d, *J* = 4.6 Hz, 2H), 7.24 (t, *J* = 8.0 Hz, 1H), 8.51 (d, *J* = 4.6 Hz, 2H). MS (ESI) *m*/*z* = 371 $[M + H]^+$.

*8-[(4-Methoxyphenyl)(pyridin-4-yl)methyl]-1,2,5,6-tetrahydro-4H-pyrrolo[3,2,1-ij]quinolin-4-one (**3k**).* The title compound was obtained according to Method B using **2k** (102 mg, 0.26 mmol), trifluoroacetic acid (0.20 mL, 2.64 mmol), triethylsilane (0.13 mL, 0.79 mmol), and trifluoromethanesulfonic acid (2 μL, 0.03 mmol) in anhydrous CH_2Cl_2 (8 mL) as pale yellow solids (83 mg, 86%), mp 71−73 °C. ^{1}H NMR

dx.doi.org/10.1021/jm301408t | *J. Med. Chem.* 2013, 56, 460−470

(500 MHz, $CDCl_3$): δ 2.66 (t, J = 7.7 Hz, 2H), 2.90 (t, J = 7.7 Hz, 2H), 3.12 (t, J = 8.4 Hz, 2H), 3.80 (s, 3H), 4.06 (t, J = 8.4 Hz, 2H), 5.38 (s, 1H), 6.71 (s, 1H), 6.78 (s, 1H), 6.85 (d, J = 8.7 Hz, 2H), 7.00 (d, J = 8.7 Hz, 2H), 7.03 (d, J = 4.7 Hz, 2H), 8.51 (d, J = 4.7 Hz, 2H). MS (ESI) m/z = 371 $[M + H]^+$. The racemate **3k** was separated by preparative HPLC on chiral stationary phase (NucleoCel Delta column, 0.8 cm × 25 cm, 50% hexane/isopropanol, 1.0 mL/min) to yield (+)-**3k** ($[\alpha]_D^{20}$ = +5.5 (c = 1.0, DMSO), 100% ee and t_R = 32.1 min by analytical HPLC, and (−)-**3k** ($[\alpha]_D^{20}$= −4.8 (c = 1.0, DMSO), 90.3% ee and t_R = 38.2 min by analytical HPLC.

*8-[(3-Fluorophenyl)(pyridin-4-yl)methyl]-1,2,5,6-tetrahydro-4H-pyrrolo[3,2,1-ij]quinolin-4-one (**3l**).* The title compound was obtained according to Method B using **2l** (96 mg, 0.26 mmol), trifluoroacetic acid (0.20 mL, 2.56 mmol), triethylsilane (0.13 mL, 0.78 mmol), and trifluoromethanesulfonic acid (2 μL, 0.03 mmol) in anhydrous CH_2Cl_2 (6 mL) as pale yellow solids (40 mg, 43%), mp 162−165 °C. ^{1}H NMR (500 MHz, $CDCl_3$): δ 2.66 (t, J = 7.7 Hz, 2H), 2.91 (t, J = 7.7 Hz, 2H), 3.14 (t, J = 8.4 Hz, 2H), 4.07 (t, J = 8.4 Hz, 2H), 5.42 (s, 1H), 6.71 (s, 1H), 6.78 (m, 2H), 6.88 (d, J = 7.7 Hz, 1H), 6.96 (td, J = 2.2, 8.3 Hz, 1H), 7.03 (d, J = 4.6 Hz, 2H), 7.29 (m, 1H), 8.53 (d, J = 4.6 Hz, 2H). MS (ESI) m/z = 359 $[M + H]^+$.

*8-[(4-Fluorophenyl)(pyridin-4-yl)methyl]-1,2,5,6-tetrahydro-4H-pyrrolo[3,2,1-ij]quinolin-4-one (**3m**).* The title compound was obtained according to Method B using **2m** (65 mg, 0.17 mmol), trifluoroacetic acid (0.13 mL, 1.74 mmol), triethylsilane (80 μL, 0.52 mmol), and trifluoromethanesulfonic acid (2 μL, 0.02 mmol) in anhydrous CH_2Cl_2 (5 mL) as pale yellow solids (45 mg, 74%), mp 155−157 °C. ^{1}H NMR (500 MHz, $CDCl_3$): δ 2.66 (t, J = 7.7 Hz, 2H), 2.90 (t, J = 7.7 Hz, 2H), 3.13 (t, J = 8.5 Hz, 2H), 4.07 (t, J = 8.5 Hz, 2H), 5.41 (s, 1H), 6.70 (s, 1H), 6.77 (s, 1H), 6.99−7.06 (m, 6H), 8.53 (dd, J = 1.6, 4.5 Hz, 2H). MS (ESI) m/z = 359 $[M + H]^+$.

*8-[(3-Chlorophenyl)(pyridin-4-yl)methyl]-1,2,5,6-tetrahydro-4H-pyrrolo[3,2,1-ij]quinolin-4-one (**3n**).* The title compound was obtained according to Method B using **2n** (85 mg, 0.22 mmol), trifluoroacetic acid (0.17 mL, 2.20 mmol), triethylsilane (0.11 mL, 0.65 mmol), and trifluoromethanesulfonic acid (2 μL, 0.02 mmol) in anhydrous CH_2Cl_2 (5 mL) as pale yellow solids (42 mg, 51%), mp 163−165 °C. ^{1}H NMR (500 MHz, $CDCl_3$): δ 2.66 (t, J = 7.7 Hz, 2H), 2.91 (t, J = 7.7 Hz, 2H), 3.14 (t, J = 8.4 Hz, 2H), 4.08 (t, J = 8.4 Hz, 2H), 5.40 (s, 1H), 6.70 (s, 1H), 6.77 (s, 1H), 6.98 (m, 1H), 7.02 (d, J = 4.6 Hz, 2H), 7.07 (s, 1H), 7.25 (m, 2H), 8.54 (d, J = 4.6 Hz, 2H). MS (ESI) m/z = 375 M^+.

*8-[(4-Chlorophenyl)(pyridin-4-yl)methyl]-1,2,5,6-tetrahydro-4H-pyrrolo[3,2,1-ij]quinolin-4-one (**3o**).* The title compound was obtained according to Method B using **2o** (95 mg, 0.24 mmol), trifluoroacetic acid (0.19 mL, 2.43 mmol), triethylsilane (0.12 mL, 0.73 mmol), and trifluoromethanesulfonic acid (3 μL, 0.02 mmol) in anhydrous CH_2Cl_2 (5 mL) as pale yellow solids (56 mg, 62%), mp 136−138 °C. ^{1}H NMR (500 MHz, $CDCl_3$): δ 2.66 (t, J = 7.7 Hz, 2H), 2.90 (t, J = 7.7 Hz, 2H), 3.13 (t, J = 8.4 Hz, 2H), 4.07 (t, J = 8.4 Hz, 2H), 5.40 (s, 1H), 6.69 (s, 1H), 6.76 (s, 1H), 7.02 (m, 4H), 7.28 (d, J = 8.5 Hz, 2H), 8.53 (d, J = 4.6 Hz, 2H). MS (ESI) m/z = 375 M^+.

*8-[(3-Methylphenyl)(pyridin-4-yl)methyl]-1,2,5,6-tetrahydro-4H-pyrrolo[3,2,1-ij]quinolin-4-one (**3p**).* The title compound was obtained according to Method B using **2p** (65 mg, 0.18 mmol), trifluoroacetic acid (0.14 mL, 1.80 mmol), triethylsilane (0.85 μL, 0.53 mmol), and trifluoromethanesulfonic acid (2 μL, 0.02 mmol) in anhydrous CH_2Cl_2 (4 mL) as pale yellow solids (32 mg, 50%), mp 180−182 °C. ^{1}H NMR (500 MHz, $CDCl_3$): δ 2.31 (s, 3H), 2.66 (t, J = 7.7 Hz, 2H), 2.90 (t, J = 7.7 Hz, 2H), 3.13 (t, J = 8.4 Hz, 2H), 4.07 (t, J = 8.4 Hz, 2H), 5.39 (s, 1H), 6.72 (s, 1H), 6.79 (s, 1H), 6.87 (d, J = 7.7 Hz, 1H), 6.91 (s, 1H), 7.04 (d, J = 4.6 Hz, 2H), 7.07 (d, J = 7.5 Hz, 1H), 7.20 (t, J = 7.6 Hz, 1H), 8.51 (d, J = 4.6 Hz, 2H). MS (ESI) m/z = 355 $[M + H]^+$.

*8-[((3,5-Bis(trifluoromethyl)phenyl)(pyridin-4-yl)methyl]-1,2,5,6-tetrahydro-4H-pyrrolo[3,2,1-ij]quinolin-4-one (**3q**).* The title compound was obtained according to Method B using **2q** (95 mg, 0.19 mmol), trifluoroacetic acid (0.15 mL, 1.93 mmol), triethylsilane (0.93 μL, 0.58 mmol), and trifluoromethanesulfonic acid (2 μL, 0.02 mmol) in anhydrous CH_2Cl_2 (6 mL) as pale yellow solids (38 mg, 42%), mp 182−184 °C. ^{1}H NMR (500 MHz, $CDCl_3$): δ 2.68 (t, J = 7.7 Hz, 2H), 2.92 (t, J = 7.7 Hz, 2H), 3.15 (t, J = 8.4 Hz, 2H), 4.09 (t, J = 8.4 Hz, 2H), 5.55 (s, 1H), 6.68 (s, 1H), 6.75 (s, 1H), 7.00 (d, J = 4.6 Hz, 2H), 7.54 (s, 2H), 7.80 (s, 1H), 8.58 (d, J = 4.6 Hz, 2H). MS (ESI) m/z = 477 $[M + H]^+$.

*8-(1-Pyridin-3-ylvinyl)-1,2,5,6-tetrahydro-4H-pyrrolo[3,2,1-ij]-quinolin-4-one (**6a**).* To a suspension of methyltriphenylphosphonium bromide (564 mg, 1.58 mmol) in anhydrous THF (25 mL) was added n-BuLi (2.5 M in hexanes, 0.58 mL, 1.44 mmol) slowly under an atmosphere of nitrogen at −78 °C. The reaction mixture was stirred at room temperature for 1 h, and then cooled to −78 °C again followed by addition of a solution of **1a** (200 mg, 0.72 mmol) in THF (5 mL). The resulting mixture was stirred at ambient temperature for 5 h and subsequently quenched with aqueous NH_4Cl, extracted with ethyl acetate (3 × 10 mL), dried over $MgSO_4$, and concentrated in vacuo. The crude product was purified by flash chromatography column on silica gel (methanol/dichloromethane, 0 to 1:70) to give off-white solids (117 mg, 59%), mp 97−99 °C. ^{1}H NMR (500 MHz, $CDCl_3$): δ 2.67 (t, J = 7.7 Hz, 2H), 2.95 (t, J = 7.7 Hz, 2H), 3.17 (t, J = 8.5 Hz, 2H), 4.10 (t, J = 8.5 Hz, 2H), 5.40 (s, 1H), 5.48 (s, 1H), 6.95 (s, 1H), 7.03 (s, 1H), 7.27 (dd, J = 4.9, 7.9 Hz, 1H), 7.61 (dt, J = 2.1, 7.9 Hz, 1H), 8.56 (dd, ^3J = 1.6, 4.8 Hz, 1H), 8.60 (d, J = 1.6 Hz, 1H). MS (ESI) m/z = 277 $[M + H]^+$.

*8-(1-Pyridin-4-ylvinyl)-1,2,5,6-tetrahydro-4H-pyrrolo[3,2,1-ij]-quinolin-4-one (**6b**).* To a suspension of methyltriphenylphosphonium bromide (564 mg, 1.58 mmol) in anhydrous THF (25 mL) was added n-BuLi (2.5 M in hexanes, 0.58 mL, 1.44 mmol) slowly under an atmosphere of nitrogen at −78 °C. The reaction mixture was stirred at room temperature for 1 h and then cooled to −78 °C again followed by addition of a solution of **1b** (200 mg, 0.72 mmol) in THF (5 mL). The resulting mixture was stirred at ambient temperature for 5 h and subsequently quenched with aqueous NH_4Cl, extracted with ethyl acetate (3 × 10 mL), dried over $MgSO_4$, and concentrated in vacuo. The crude product was purified by flash chromatography column on silica gel (methanol/dichloromethane, 0 to 1:50) to give pale yellow semisolids (115 mg, 58%). ^{1}H NMR (500 MHz, $CDCl_3$): δ 2.69 (t, J = 7.7 Hz, 2H), 2.95 (t, J = 7.7 Hz, 2H), 3.18 (t, J = 8.5 Hz, 2H), 4.10 (t, J = 8.5 Hz, 2H), 5.51 (d, J = 8.1 Hz, 2H), 6.93 (s, 1H), 7.00 (s, 1H), 7.23 (dd, J = 1.6, 4.5 Hz, 2H), 8.58 (dd, J = 1.5, 4.6 Hz, 2H). MS (ESI) m/z = 277 $[M + H]^+$.

*8-(1-Pyridin-3-ylethyl)-1,2,5,6-tetrahydro-4H-pyrrolo[3,2,1-ij]-quinolin-4-one (**7a**).* To a solution of **6a** (59 mg, 0.21 mmol) in methanol (8 mL) was added 5% Pd/C (9 mg). Subsequently, the reaction was stirred under a hydrogen atmosphere (maintained with balloons) for 10 h followed by filtration through a Celite cake and concentration in vacuo. The crude product was purified by flash chromatography column on silica gel (methanol/dichloromethane, 0 to 1:50) to give white solids (36 mg, 62%), mp 100−102 °C. ^{1}H NMR (500 MHz, $CDCl_3$): δ 1.64 (d, J = 7.2 Hz, 3H), 2.65 (t, J = 7.8 Hz, 2H), 2.92 (t, J = 7.8 Hz, 2H), 3.14 (t, J = 8.4 Hz, 2H), 4.06 (t, J = 8.4 Hz, 2H), 4.11 (q, J = 7.2 Hz, 1H), 6.83 (s, 1H), 6.91 (s, 1H), 7.21 (dd, J = 4.7, 7.9 Hz, 1H), 7.49 (dt, J = 1.8, 7.9 Hz, 1H), 8.44 (dd, J = 1.5, 4.7 Hz, 1H), 8.51 (d, J = 2.2 Hz, 1H). MS (ESI) m/z = 279 $[M + H]^+$.

*8-(1-Pyridin-4-ylethyl)-1,2,5,6-tetrahydro-4H-pyrrolo[3,2,1-ij]-quinolin-4-one (**7b**).* To a solution of **6b** (115 mg, 0.38 mmol) in methanol (8 mL) was added 5% Pd/C (16 mg). Subsequently, the reaction was stirred under a hydrogen atmosphere (maintained with balloons) for 10 h followed by filtration through a Celite cake and concentration in vacuo. The crude product was purified by flash chromatography column on silica gel (methanol/dichloromethane, 0 to 1:50) to give off-white solids (84 mg, 79%), mp 103−105 °C. ^{1}H NMR (500 MHz, $CDCl_3$): δ 1.61 (d, J = 7.2 Hz, 3H), 2.66 (t, J = 7.8 Hz, 2H), 2.92 (t, J = 7.8 Hz, 2H), 3.14 (t, J = 8.4 Hz, 2H), 4.06 (m, 3H), 6.81 (s, 1H), 6.90 (s, 1H), 7.13 (dd, J = 1.3, 4.8 Hz, 2H), 8.50 (dd, J = 1.3, 4.8 Hz, 2H). MS (ESI) m/z = 279 $[M + H]^+$.

Docking Study. *Crystal Processing.* Hydrogens and partial charges were added via Protonate3D application in MOE 2008.

Ligands. Compounds were built and energy minimized in the MMFF94s force field with MOE 2008. No conformation search was performed, because the docking software GOLD automatically generates them.

Docking. The automatic active-site detection was switched on, while heme iron was selected as active-site origin and the radius of active site

was set to 19 Å. A distance constraint of 1.9−2.5 Å between the sp^2 hybrid N and the iron was set as well. Ligand was docked in 50 independent genetic algorithm (GA) iterations for each of the three GOLD-docking runs. Moreover, the goldscore.p450_pdb parameters were exploited, and the genetic algorithm default parameters were set. The resulting poses were subsequently ranked according to fitness and further evaluated with LigX module in MOE 2008.

■ ASSOCIATED CONTENT

Supporting Information

The experimental details and characterization of compounds **4a**, **4b**, and intermediates **2a−2g** and **2i−2q**, the ^{13}C NMR and HPLC purities of all final compounds, and docking results of both enantiomers of compound **3k** in CYP19. This material is available free of charge via the Internet at http://pubs.acs.org.

■ AUTHOR INFORMATION

Corresponding Author

*Phone: +(49) 681 302 70300. Fax: +(49) 681 302 70308. E-mail: rolf.hartmann@helmholtz-hzi.de. Homepage: http://www.helmholtz-hzi.de/?id=3897.

Notes

The authors declare no competing financial interest.

■ ACKNOWLEDGMENTS

The authors thank Dr. Jörg Haupenthal, Dr. Christina Zimmer, Jeannine Jung, and Jannine Ludwig for their help in performing the *in vitro* test, as well as Dr. Stefan Boettcher, Frauke Maurer, and Michael Zender for chiral separation and ee determination. The authors also appreciate Professor Hermans (University of Maastricht, The Netherlands) for providing us with V79MZh11B1 cells expressing human CYP11B1.

■ ABBREVIATIONS USED:

BC, breast cancer; CYP, cytochrome P450; ER, estrogen receptor; PgR, progesterone receptor; CYP19, aromatase, estrogen synthase; CVD, cardiovascular disease; CYP11B2, aldosterone synthase; ROS, reactive oxygen species; CYP17, 17α-hydroxylase-17,20-lyase; CYP11B1, 11β-hydroxylase; DMA, *N*,*N*-dimethylacetamide; NBS, *N*-bromosuccinimide; SF, selectivity factor = IC_{50}(CYP11B1)/IC_{50}(CYP11B2)

■ REFERENCES

(1) Miller, W. R. Endocrine treatment for breast cancers: Biological rationale and current progress. *J. Steroid Biochem. Mol. Biol.* **1990**, *37*, 467−480.

(2) Wang, T.; You, Q.; Huang, F. S.; Xiang, H. Recent advances in selective estrogen receptor modulators for breast cancer. *Mini-Rev. Med. Chem.* **2009**, *9*, 1191−1201.

(3) (a) American Heart Association. *Heart disease and stroke statistics: 2004 update*; American Heart Association: Dallas, TX, 2003. (b) Witteman, J. C.; Grobbee, D. E.; Kok, F. J.; Hofman, A.; Valkenburg, H. A. Increased risk of atherosclerosis in women after the menopause. *Br. Med. J.* **1989**, *298*, 642−644.

(4) Booth, E. A.; Marchesi, M.; Kilbourne, E. J.; Lucchesi, B. R. 17β-Estradiol as a receptor-mediated cardioprotective agent. *J. Pharmacol. Exp. Ther.* **2003**, *307*, 395−401.

(5) Arias-Loza, P. A.; Muehlfelder, M.; Elmore, S. A.; Maronpot, R.; Hu, K.; Blode, H.; Hegele-Hartung, C.; Fritzemeier, K. H.; Ertl, G.; Pelzer, T. Differential effects of 17β-estradiol and of synthetic progestins on aldosterone-salt-induced kidney disease. *Toxicol. Pathol.* **2009**, *37*, 969−982.

(6) Beer, S.; Reincke, M.; Kral, M.; Callies, F.; Ströer, H.; Dienesch, C.; Steinhauer, S.; Ertl, G.; Allolio, B.; Neubauer, S. High-dose 17β-estradiol treatment prevents development of heart failure post-myocardial infarction in the rat. *Basic Res. Cardiol.* **2007**, *102*, 9−18.

(7) Gardner, J. D.; Murray, D. B.; Voloshenyuk, T. G.; Brower, G. L.; Bradley, J. M.; Janicki, J. S. Estrogen attenuates chronic volume overload induced structural and functional remodeling in male rat hearts. *Am. J. Physiol.: Heart Circ. Physiol.* **2010**, *298*, H497−H504.

(8) Jurgen, G.; Ben, H.; Gun, A.; Mitch, D.; Per Eystein, L. Influence of letrozole and anastrozole on total body aromatization and plasma estrogen levels in postmenopausal breast cancer patients evaluated in a randomized, cross-over study. *J. Clin. Oncol.* **2002**, *20*, 751−757.

(9) (a) Fischer, M.; Baessler, A.; Schunkert, H. Renin angiotensin system and gender differences in the cardiovascular system. *Cardiovasc. Res.* **2002**, *53*, 672−677. (b) Roesch, D. M.; Tian, Y.; Zheng, W.; Shi, M.; Verbalis, J. G.; Sandberg, K. Estradiol attenuates angiotensin-induced aldosterone secretion in ovariectomized rats. *Endocrinology* **2000**, *141*, 4629−4636. (c) Chappell, M. C.; Gallagher, P. E.; Averill, D. B.; Ferrario, C. M.; Brosnihan, K. B. Estrogen or the AT1 antagonist olmesartan reverses the development of profound hypertension in the congenic mRen2.Lewis rat. *Hypertension* **2003**, *42*, 781−786.

(10) Duprez, D. A. Aldosterone and the vasculature: Mechanisms mediating resistant hypertension. *J. Clin. Hypertens.* **2007**, *9*, 13−18.

(11) Romagni, P.; Rossi, F.; Guerrini, L.; Quirini, C.; Santiemma, V. Aldosterone induces contraction of the resistance arteries in man. *Atherosclerosis* **2003**, *166*, 345−349.

(12) Fejes-Tóth, G.; Náray-Fejes-Tóth, A. Early aldosterone-regulated genes in cardiomyocytes: Clues to cardiac remodeling? *Endocrinology* **2007**, *148*, 1502−1510.

(13) Joffe, H. V.; Adler, G. K. Effect of aldosterone and mineralocorticoid receptor blockade on vascular inflammation. *Heart Failure Rev.* **2005**, *10*, 31−37.

(14) Fiebeler, A.; Luft, F. C. The mineralocorticoid receptor and oxidative stress. *Heart Failure Rev.* **2005**, *10*, 47−52.

(15) (a) Leibovitz, E.; Ebrahimian, T.; Paradis, P.; Schiffrin, E. L. Aldosterone induces arterial stiffness in absence of oxidative stress and endothelial dysfunction. *J. Hypertens.* **2009**, *27*, 2192−2200. (b) Weber, K. T.; Brilla, C. G.; Campbell, S. E.; Guarda, E.; Zhou, G.; Sriram, K. Myocardial fibrosis: Role of angiotensin II and aldosterone. *Basic Res. Cardiol.* **1993**, *88*, 107−124.

(16) Qin, W.; Rudolph, A. E.; Bond, B. R.; Rocha, R.; Blomme, E. A. G.; Goellner, J. J.; Funder, J. W.; McMahon, E. G. Transgenic model of aldosterone-driven cardiac hypertrophy and heart failure. *Circ. Res.* **2003**, *93*, 69−76.

(17) (a) Morphy, R.; Rankovic, Z. Designed multiple ligands. An emerging drug discovery paradigm. *J. Med. Chem.* **2005**, *48*, 6523−6543. (b) Cavalli, A.; Bolognesi, M. L.; Minarini, A.; Rosini, M.; Tumiatti, V.; Recanatini, M.; Melchiorre, C. Multi-target-directed ligands to combat neurodegenerative diseases. *J. Med. Chem.* **2008**, *51*, 347−372. (c) Morphy, R. Selectively nonselective kinase inhibition: Striking the right balance. *J. Med. Chem.* **2010**, *53*, 1413−1437.

(18) (a) Hartmann, R. W.; Bayer, H.; Grün, G. Aromatase inhibitors. Syntheses and structure-activity studies of novel pyridyl-substituted indanones, indans, and tetralins. *J. Med. Chem.* **1994**, *37*, 1275−1281. (b) Gobbi, S.; Cavalli, A.; Rampa, A.; Belluti, F.; Piazzi, L.; Paluszcak, A.; Hartmann, R. W.; Recanatini, M.; Bisi, A. Lead optimization providing a series of flavone derivatives as potent nonsteroidal inhibitors of the cytochrome P450 aromatase enzyme. *J. Med. Chem.* **2006**, *49*, 4777−4780. (c) Abadi, A. H.; Abou-Seri, S. M.; Hu, Q.; Negri, M.; Hartmann, R. W. Synthesis and biological evaluation of imidazolylmethylacridones as cytochrome P-450 enzymes inhibitors. *Med. Chem. Commun.* **2012**, *3*, 663−666. (d) Le Borgne, M.; Marchand, P.; Duflos, M.; Delevoye-Seiller, B.; Piessard-Robert, S.; Le Baut, G.; Hartmann, R. W.; Palzer, M. Synthesis and in vitro evaluation of 3-(1-azolylmethyl)-1H-indoles and 3-(1-azoly1-1-phenylmethyl)-1H-indoles as inhibitors of P450 arom. *Arch. Pharm. (Weinheim, Ger.)* **1997**, *330*, 141−145. (e) Woo, L. W. L.; Jackson, T.; Putey, A.; Cozier, G.; Leonard, P.; Acharya, K. R.; Chander, S. K.; Purohit, A.; Reed, M. J.; Potter, B. V. L Highly potent first examples of dual aromatase-steroid sulfatase inhibitors based on a biphenyl template. *J. Med. Chem.* **2010**, *53*, 2155−2170. (f) Leze, M. P.; Le Borgne, M.; Pinson, P.; Palusczak, A.; Duflos, M.; Le Baut, G.;

Hartmann, R. W. Synthesis and biological evaluation of 5-[(aryl)(1H-imidazol-1-yl)methyl]-1H-indoles: potent and selective aromatase inhibitors. *Bioorg. Med. Chem. Lett.* **2006**, *16*, 1134−1137. (g) Gobbi, S.; Cavalli, A.; Negri, M.; Schewe, K. E.; Belluti, F.; Piazzi, L.; Hartmann, R. W.; Recanatini, M.; Bisi, A. Imidazolylmethylbenzophenones as highly potent aromatase inhibitors. *J. Med. Chem.* **2007**, *50*, 3420−3422. (h) Al-Soud, Y. A.; Heydel, M.; Hartmann, R. W. Design and synthesis of 1,3,5-trisubstituted 1,2,4-triazoles as CYP enzyme inhibitors. *Tetrahedron Lett.* **2011**, *52*, 6372−6375. (i) Leonetti, F.; Favia, A.; Rao, A.; Aliano, R.; Paluszcak, A.; Hartmann, R. W.; Carotti, A. Design, synthesis, and 3D QSAR of novel potent and selective aromatase inhibitors. *J. Med. Chem.* **2004**, *47*, 6792−6803. (j) Stefanachi, A.; Favia, A. D.; Nicolotti, O.; Leonetti, F.; Pisani, L.; Catto, M.; Zimmer, C.; Hartmann, R. W.; Carotti, A. Design, synthesis, and biological evaluation of imidazolyl derivatives of 4,7-disubstituted coumarins as aromatase inhibitors selective over 17-α-hydroxylase/C17-20 lyase. *J. Med. Chem.* **2011**, *54*, 1613−1625.

(19) (a) Hu, Q.; Negri, M.; Jahn-Hoffmann, K.; Zhuang, Y.; Olgen, S.; Bartels, M.; Müller-Vieira, U.; Lauterbach, T.; Hartmann, R. W. Synthesis, biological evaluation, and molecular modeling studies of methylene imidazole substituted biaryls as inhibitors of human 17α-hydroxylase-17,20-lyase (CYP17)-Part II: Core rigidification and influence of substituents at the methylene bridge. *Bioorg. Med. Chem.* **2008**, *16*, 7715−7727. (b) Hille, U. E.; Hu, Q.; Vock, C.; Negri, M.; Bartels, M.; Müller-Vieira, U.; Lauterbach, T.; Hartmann, R. W. Novel CYP17 inhibitors: Synthesis, biological evaluation, structure-activity relationships and modeling of methoxy- and hydroxy-substituted methyleneimidazolyl biphenyls. *Eur. J. Med. Chem.* **2009**, *44*, 2765−2775. (c) Hu, Q.; Negri, M.; Olgen, S.; Hartmann, R. W. The role of fluorine substitution in biphenyl methylene imidazole type CYP17 inhibitors for the treatment of prostate carcinoma. *ChemMedChem* **2010**, *5*, 899−910. (d) Hu, Q.; Jagusch, C.; Hille, U. E.; Haupenthal, J.; Hartmann, R. W. Replacement of imidazolyl by pyridyl in biphenyl methylenes results in selective CYP17 and dual CYP17/CYP11B1 inhibitors for the treatment of prostate cancer. *J. Med. Chem.* **2010**, *53*, 5749−5758. (e) Hu, Q.; Yin, L.; Jagusch, C.; Hille, U. E.; Hartmann, R. W. Isopropylidene substitution increases activity and selectivity of biphenyl methylene 4-pyridine type CYP17 inhibitors. *J. Med. Chem.* **2010**, *53*, 5049−5053. (f) Pinto-Bazurco Mendieta, M. A. E.; Negri, M.; Hu, Q.; Hille, U. E.; Jagusch, C.; Jahn-Hoffmann, K.; Müller-Vieira, U.; Schmidt, D.; Lauterbach, T.; Hartmann, R. W. CYP17 inhibitors. Annulations of additional rings in methylene imidazole substituted biphenyls: synthesis, biological evaluation and molecular modeling. *Arch. Pharm. (Weinheim, Ger.)* **2008**, *341*, 597−609. (g) Hille, U. E.; Hu, Q.; Pinto-Bazurco Mendieta, M. A. E.; Bartels, M.; Vock, C. A.; Lauterbach, T.; Hartmann, R. W. Steroidogenic cytochrome P450 (CYP) enzymes as drug targets: Combining substructures of known CYP inhibitors leads to compounds with different inhibitory profile. *C. R. Chim.* **2009**, *12*, 1117−1126. (h) Jagusch, C.; Negri, M.; Hille, U. E.; Hu, Q.; Bartels, M.; Jahn-Hoffmann, K.; Pinto-Bazurco Mendieta, M. A. E.; Rodenwaldt, B.; Müller-Vieira, U.; Schmidt, D.; Lauterbach, T.; Recanatini, M.; Cavalli, A.; Hartmann, R. W. Synthesis, biological evaluation and molecular modeling studies of methyleneimidazole substituted biaryls as inhibitors of human 17α-hydroxylase-17,20-lyase (CYP17) − Part I: heterocyclic modifications of the core structure. *Bioorg. Med. Chem.* **2008**, *16*, 1992−2010. (i) Krug, S. J.; Hu, Q.; Hartmann, R. W. Hits identified in library screening demonstrate selective CYP17A1 lyase inhibition. *J. Steroid Biochem. Mol. Biol.* **2013**, *134*, 75−79.

(20) (a) Hille, U. E.; Zimmer, C.; Vock, C. A.; Hartmann, R. W. Discovery of the first selective steroid-11β-hydroxylase (CYP11B1) inhibitors for the treatment of cortisol dependent diseases. *ACS Med. Chem. Lett.* **2011**, *2*, 2−6. (b) Hille, U. E.; Zimmer, C.; Haupenthal, J.; Hartmann, R. W. Optimization of the first selective steroid-11β-hydroxylase (CYP11B1) inhibitors for the treatment of cortisol dependent diseases. *ACS Med. Chem. Lett* **2011**, *2*, 559−564. (c) Zolle, I. M.; Berger, M. L.; Hammerschmidt, F.; Hahner, S.; Schirbel, A.; Peric-Simov, B. New selective inhibitors of steroid 11β-hydroxylation in the adrenal cortex: Synthesis and structure-activity relationship of potent etomidate analogues. *J. Med. Chem.* **2008**, *51*, 2244−2253. (d) Yin, L.; Lucas, S.; Maurer, F.; Kazmaier, U.; Hu, Q.; Hartmann, R. W. Novel imidazol-1-ylmethyl substituted 1,2,5,6-tetrahydro-pyrrolo[3,2,1-*ij*]quinolin-4-ones as potent and selective CYP11B1 inhibitors for the treatment of Cushing's syndrome. *J. Med. Chem.* **2012**, *55*, 6629−6633.

(21) (a) Lucas, S.; Heim, R.; Ries, C.; Schewe, K. E.; Birk, B.; Hartmann, R. W. In vivo active aldosterone synthase inhibitors with improved selectivity: Lead optimization providing a series of pyridine substituted 3,4-dihydro-1*H*-quinolin-2-one derivatives. *J. Med. Chem.* **2008**, *51*, 8077−8087. (b) Lucas, S.; Heim, R.; Negri, M.; Antes, I.; Ries, C.; Schewe, K. E.; Bisi, A.; Gobbi, S.; Hartmann, R. W. Novel aldosterone synthase inhibitors with extended carbocyclic skeleton by a combined ligand-based and structure-based drug design approach. *J. Med. Chem.* **2008**, *51*, 6138−6149. (c) Heim, R.; Lucas, S.; Grombein, C. M.; Ries, C.; Schewe, K. E.; Negri, M.; Müller-Vieira, U.; Birk, B.; Hartmann, R. W. Overcoming undesirable CYP1A2 inhibition of pyridylnaphthalene-type aldosterone synthase inhibitors: influence of heteroaryl derivatization on potency and selectivity. *J. Med. Chem.* **2008**, *51*, 5064−5074. (d) Voets, M.; Antes, I.; Scherer, C.; Müller-Vieira, U.; Biemel, K.; Marchais-Oberwinkler, S.; Hartmann, R. W. Synthesis and evaluation of heteroaryl-substituted dihydronaphthalenes and indenes: potent and selective inhibitors of aldosterone synthase (CYP11B2) for the treatment of congestive heart failure and myocardial fibrosis. *J. Med. Chem.* **2006**, *49*, 2222−2231. (e) Voets, M.; Antes, I.; Scherer, C.; Müller-Vieira, U.; Biemel, K.; Barassin, C.; Marchais-Oberwinkler, S.; Hartmann, R. W. Heteroaryl-substituted naphthalenes and structurally modified derivatives: Selective inhibitors of CYP11B2 for the treatment of congestive heart failure and myocardial fibrosis. *J. Med. Chem.* **2005**, *48*, 6632−6642. (f) Ulmschneider, S.; Müller-Vieira, U.; Klein, C. D.; Antes, I.; Lengauer, T.; Hartmann, R. W. Synthesis and evaluation of (pyridylmethylene) tetrahydronaphthalenes/-indanes and structurally modified derivatives: Potent and selective inhibitors of aldosterone synthase. *J. Med. Chem.* **2005**, *48*, 1563−1575. (g) Ulmschneider, S.; Müller-Vieira, U.; Mitrenga, M.; Hartmann, R. W.; Oberwinkler-Marchais, S.; Klein, C. D.; Bureik, M.; Bernhardt, R.; Antes, I.; Lengauer, T. Synthesis and evaluation of imidazolylmethylene tetrahydronaphthalenes and imidazolylmethyleneindanes: potent inhibitors of aldosterone synthase. *J. Med. Chem.* **2005**, *48*, 1796−1805. (h) Lucas, S.; Negri, M.; Heim, R.; Zimmer, C.; Hartmann, R. W. Fine-tuning the selectivity of aldosterone synthase inhibitors: Insights from studies from studies of heteroaryl substituted 1,2,5,6-tetrahydropyrrolo[3,2,1-*ij*]-quinoline-4-one derivatives. *J. Med. Chem.* **2011**, *54*, 2307−2319. (i) Yin, L.; Hu, Q.; Hartmann, R. W. 3-Pyridinyl substituted aliphatic cycles as CYP11B2 inhibitors: aromaticity abolishment of the core significantly increased selectivity over CYP1A2. *PLoS ONE* **2012**, *7* (11), No. e48048, DOI: 10.1371/journal.pone.0048048. (j) Hu, Q.; Yin, L.; Hartmann, R. W. Selective dual inhibitors of CYP19 and CYP11B2: Targeting cardiovascular diseases hiding in the shadow of breast cancer. *J. Med. Chem.* **2012**, *55*, 7080−7089.

(22) (a) Hartmann, R. W.; Batzl, C. Aromatase inhibitors. Synthesis and evaluation of mammary tumor inhibiting activity of 3-alkylated 3-(4-aminophenyl)piperidine-2,6-diones. *J. Med. Chem.* **1986**, *29*, 1362−1369. (b) Denner, K.; Doehmer, J.; Bernhardt, R. Cloning of CYP11B1 and CYP11B2 from normal human adrenal and their functional expression in COS-7 and V79 chinese hamster cells. *Endocr. Res.* **1995**, *21*, 443−448. (c) Ehmer, P. B.; Bureik, M.; Bernhardt, R.; Müller, U.; Hartmann, R. W. Development of a test system for inhibitors of human aldosterone synthase (CYP11B2): Screening in fission yeast and evaluation of selectivity in V79 cells. *J. Steroid Biochem. Mol. Biol.* **2002**, *81*, 173−179. (d) Ehmer, P. B.; Jose, J.; Hartmann, R. W. Development of a simple and rapid assay for the evaluation of inhibitors of human 17α-hydroxylase-C(17,20)-lyase (P450c17) by coexpression of P450c17 with NADPH-cytochrome-P450-reductase in *Escherichia coli*. *J. Steroid Biochem. Mol. Biol.* **2000**, *75*, 57−63. (e) Hutschenreuter, T. U.; Ehmer, P. E.; Hartmann, R. W. Synthesis of hydroxy derivatives of highly potent non-steroidal CYP 17 Inhibitors as potential metabolites and evaluation of their activity by a non cellular assay using recombinant human enzyme. *J. Enzyme Inhib. Med. Chem.* **2004**, *19*, 17−32.